KSHV LANA acetylation-selective acidic domain reader sequence mediates virus persistence

Franceline Juillard[a,1], Marta Pires de Miranda[b,1], Shijun Li[a], Aura Franco[b], André F. Seixas[b], Bing Liu[a], Ángel L. Álvarez[a], Min Tan[a], Agnieszka Szymula[a], Kenneth M. Kaye[a,2,3], and J. Pedro Simas[b,c,2,3]

[a]Departments of Medicine, Brigham and Women's Hospital and Harvard Medical School, Boston, MA 02115; [b]Instituto de Medicina Molecular, Faculdade de Medicina, Universidade de Lisboa, 1649-028 Lisboa, Portugal; and [c]Institute of Health Sciences, Universidade Católica Portuguesa, 1649-023 Lisboa, Portugal

Edited by Yuan Chang, University of Pittsburgh, Pittsburgh, PA, and approved July 20, 2020 (received for review March 13, 2020)

Viruses modulate biochemical cellular pathways to permit infection. A recently described mechanism mediates selective protein interactions between acidic domain readers and unacetylated, lysine-rich regions, opposite of bromodomain function. Kaposi´s sarcoma (KS)-associated herpesvirus (KSHV) is tightly linked with KS, primary effusion lymphoma, and multicentric Castleman's disease. KSHV latently infects cells, and its genome persists as a multicopy, extrachromosomal episome. During latency, KSHV expresses a small subset of genes, including the latency-associated nuclear antigen (LANA), which mediates viral episome persistence. Here we show that LANA contains two tandem, partially overlapping, acidic domain sequences homologous to the SET oncoprotein acidic domain reader. This domain selectively interacts with unacetylated p53, as evidenced by reduced LANA interaction after overexpression of CBP, which acetylates p53, or with an acetylation mimicking carboxyl-terminal domain p53 mutant. Conversely, the interaction of LANA with an acetylation-deficient p53 mutant is enhanced. Significantly, KSHV LANA mutants lacking the acidic domain reader sequence are deficient for establishment of latency and persistent infection. This deficiency was confirmed under physiological conditions, on infection of mice with a murine gammaherpesvirus 68 chimera expressing LANA, where the virus was highly deficient in establishing latent infection in germinal center B cells. Therefore, LANA's acidic domain reader is critical for viral latency. These results implicate an acetylation-dependent mechanism mediating KSHV persistence and expand the role of acidic domain readers.

Kaposi´s sarcoma herpesvirus | latency-associated nuclear antigen | virus persistence | acetylation-regulated interaction | acidic domain reader

Lysine acetylation is emerging as an important posttranslational modification that regulates the function of proteins as well as histones. Acetylation is determined through a dynamic interplay between acetyltransferases and deacetylases. Bromodomains and acidic domains containing proteins typified by the SET oncoprotein are readers of acetylated and unacetylated ligands, respectively. Perhaps the best-characterized acetylation-dependent regulation of a nonhistone protein is of tumor-suppressor protein p53 (1). Phosphorylation at N-terminal p53 allows recruitment of the closely related cotranscription factors CBP/p300, which can acetylate lysine residues in the p53 carboxyl-terminal domain. Complexes of p53 and CBP/p300 recognize specific promoter sequences to initiate the transcription of p53-targeted genes. Bromodomains, such as those present in CBP/p300, interact with acetylated lysines by structurally forming a hydrophobic pocket (2). Conversely, acidic domain readers bind to positively charged unacetylated clusters of lysines. p53-SET complexes bind to p53-targeted promoters, blocking transcription (3). Therefore, p53-driven transcription is regulated through an interplay between bromodomain acetylation-dependent activation and acidic domain unacetylated-dependent repression.

Kaposi's sarcoma (KS)-associated herpesvirus (KSHV) is etiologically linked to KS, primary effusion lymphoma, and multicentric Castleman's disease (4–7). During latent infection of B cells, KSHV expresses a limited number of proteins, including the latency-associated nuclear antigen (LANA) (8). LANA is a 1,162 amino acid protein with an N-terminal proline-rich region, a C-terminal region containing a DNA-binding domain, and extensive central repetitive sequence, including an aspartic and glutamic acid rich region (Fig. 1).

A critical function of LANA is mediation of viral episome persistence by mediating the replication and tethering of viral genomes to host mitotic chromosomes to allow segregation to progeny nuclei during latent infection of proliferating cells (15–18). Some molecular aspects of this function are well characterized. LANA amino acids 5 to 13 encode a chromosome-binding motif that binds histones H2A/H2B (11). The C-terminal LANA region self-associates to bind chromatin and recognizes specific DNA sequences within the terminal repeat (TR) region of KSHV episomes. In addition to episomal persistence, other functions have been ascribed to LANA, including transcriptional activity and growth effects on the cell. An example is inhibition of host nuclear factor-kappa B (NF-κB) transcriptional activity through polyubiquitination and subsequent proteasomal-dependent

Significance

Understanding how viruses modulate host cell function is central to prospects for potential therapies. A recently described mechanism mediates selective protein interactions between acidic domain readers and unacetylated, lysine-rich regions, opposite of bromodomain function. Here we show that the latency-associated nuclear antigen (LANA) encoded by Kaposi´s sarcoma-associated herpesvirus (KSHV) contains a SET oncoprotein homologous acidic domain reader that interacts with p53 in an acetylation-dependent manner. Significantly, the LANA acidic domain reader is critical for viral latency and persistent infection. The finding that KSHV has evolved a mechanism for acetylation-dependent protein interaction underscores the physiological importance of this cellular regulatory posttranslational modification. Furthermore, opportunity may exist to develop inhibitors that disrupt LANA acidic domain reader function for therapy of KSHV-associated tumors.

Author contributions: F.J., M.P.d.M., S.L., K.M.K., and J.P.S. designed research; F.J., M.P.d.M., S.L., A.F., A.F.S., B.L., Á.L.Á., M.T., and A.S. performed research; F.J., M.P.d.M., S.L., A.F., A.F.S., B.L., Á.L.Á., M.T., A.S., K.M.K., and J.P.S. analyzed data; and F.J., M.P.d.M., K.M.K., and J.P.S. wrote the paper.

The authors declare no competing interest.

This article is a PNAS Direct Submission.

This open access article is distributed under Creative Commons Attribution-NonCommercial-NoDerivatives License 4.0 (CC BY-NC-ND).

[1]F.J. and M.P.d.M. contributed equally to this work.

[2]K.M.K. and J.P.S. contributed equally to this work.

[3]To whom correspondence may be addressed. Email: kkaye@bwh.harvard.edu or psimas@medicina.ulisboa.pt.

This article contains supporting information online at https://www.pnas.org/lookup/suppl/doi:10.1073/pnas.2004809117/-/DCSupplemental.

First published August 20, 2020.

Downloaded at Universidade Católica Portuguesa on November 13, 2020

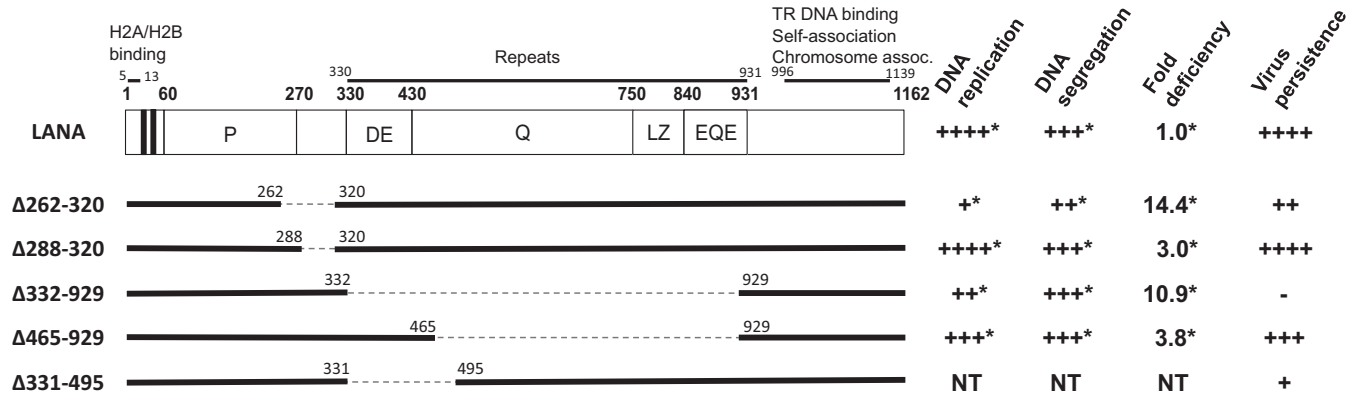

Fig. 1. Schematic representation of KSHV LANA and LANA mutants. The amino terminal bipartite nuclear localization signal (NLS) at residues 24 to 30 and 41 to 47 (9, 10) is indicated by the two vertical black bands. LANA regions identified include proline-rich (P), aspartate- and glutamate-rich (DE), glutamine-rich (Q), glutamate- and glutamine-rich (EQE), and putative leucine zipper (LZ). The DE, Q, LZ, and EQE regions each contain imperfect repeat elements. Residues 5 to 13 mediate chromosome association through interaction with histones H2A/H2B (11, 12). Residues 996 to 1,139 bind TR DNA, mediate self-association, and associate with mitotic chromosomes. The capabilities for DNA replication, episome segregation, LANA mediated episome persistence, and KSHV persistence in cells are summarized at the right. *Data from refs. 13 and 14. NT, not tested.

nuclear degradation of the NF-κB family member p65/RelA (19, 20). This mechanism involves the assembly of an ElonginC/Cullin5/SOCS (suppressors of cytokine signaling)-like complex, mediated by an unconventional viral SOCS-box motif present in LANA. The related murine gammaherpesvirus 68 (MHV-68) LANA has an EC5S that also targets cellular control of Myc turnover by antagonizing SCF(Fbw7)-mediated proteasomal degradation of Myc, mimicking SCF(β-TrCP) (21). However, much remains to be defined regarding how LANA interacts with cellular proteins to exert its functions.

Here we show that LANA contains two tandem, partially overlapping acidic domain sequences, homologous to the SET acidic domain reader sequence. This domain mimics SET's preferential binding of the unacetylated p53 C-terminal domain. Viruses lacking the acidic domain reader were deficient in establishing latent infection and virus persistence, including in germinal center B cells. Therefore, LANA's acidic domain reader is a key element mediating virus persistence and likely KSHV-associated oncogenesis.

Materials and Methods

Cell Lines. 293T cells were maintained in DMEM (Corning) supplemented with 10% bovine growth serum (GE Healthcare) and 15 ug/mL gentamicin (Gemini). Baby hamster kidney (BHK-21) fibroblasts were maintained in GMEM (Gibco) supplemented with 10% fetal bovine serum (Gibco), 50 U/mL penicillin, 50 ug/mL streptomycin (Gibco), 2 mM L-glutamine (Gibco), and 10% tryptose phosphate broth (TPB) (Sigma-Aldrich). NIH 3T3-CRE cells were maintained in DMEM (Gibco) supplemented as for BHK-21 cells without TPB (22).

Plasmids and BACs. pT7LANA, pT7LANAΔ262–320, pT7LANAΔ288–320, pT7LANAΔ332–929, and pT7LANAΔ465–929 have been described previously (13, 14). HA-CBP (23) was a gift from Wei Gu, Columbia University. BAC16(21)and pEPCMV-in (24) were gifts from Jae Jung, University of Southern California. pcDNA3 flag p53 was generated by Thomas Roberts and obtained from Addgene (25). To generate pEGFP-NLS-LANA 275–435, GFP LANA 274–777 (26) was digested with AclI (located at LANA codon 435) and BamHI (located immediately downstream of the LANA ORF in the polylinker.) Oligonucleotides 5′-CGTGATAAATCAGCTGATAACCCTGTTCGAGA GCTACGTCGTAGCG-3′ and 5′-**GATCC**GCTACGACGTAGCTCTCGAACAGGGTT ATCAGCTGATTTATCA-3′ were annealed to generate a linker with a 5′ compatible AclI overhang (indicated in italics) and a 3′ compatible BamHI overhang (indicated in bold). Stop codons immediately following the AclI overhang are underscored. The linker was ligated with AclI/BamHI-digested GFP LANA 274–777 to generate pEGFP-NLS-LANA 275–435.

BACΔLANA was generated by removing LANA from BAC16 as follows. The kanamycin resistance in pEPCMV-in was amplified by PCR using the primers 5′-**AATGCGCCTGAGGTCGGGACGGAGCACCGGCGCGCCCTTAACGAG AG**agccacacctctccccctttttcctTAGGGATAACAGGGTAATCGATTTATTC- 3′ and 5′-gcggcgacggtggcttctagggaggaaaaaggggagaggtgtggct**CTCTCGTTAAGG GCGCGCCGGTGCT**TGCTAGCCAGTGTTACAACCAATTAACC-3′ **(**LANA sequences in bold, BAC16 sequences lowercase, kanamycin cassette sequence underscored). The PCR fragment was then recombined into BAC16 in the LANA gene as described previously (24) (*SI Appendix*, Fig. S1, *Left*). In brief, PCR- amplified DNA was electroporated using a BTX *Escherichia coli* TransPorator (1.8 kV, 0.1-cm cuvette) into GS1783 *E. coli* cells (a gift from Jae Jung) containing BAC16. The bacteria transiently expressed the proteins gam, bet, and exo, which are temperature-inducible in GS1783 cells. These proteins are necessary for the homologous recombination of linear DNA fragments. Clones were selected for kanamycin resistance, and the deletion of LANA was verified by PCR and by sequencing of the PCR products. NheI restriction enzyme digestion confirmed the absence of the LANA containing BAC DNA fragment in BACΔLANA (*SI Appendix*, Fig. S2 *A* and *B*).

The kanamycin resistance was subsequently removed in a "scarless" fashion as described previously (24). In brief, the arabinose-inducible gene encoding the I-SceI enzyme was expressed following 1% arabinose treatment, resulting in linearization of the BAC by cleavage in the kanamycin gene. Following linearization, the BAC was recircularized by transient induction of gam, bet, and exo to enable recombination between duplicated sequences flanking the kanamycin cassette, resulting in kanamycin loss from the BAC (*SI Appendix*, Fig. S1, *Left*). Kanamycin-sensitive clones were then identified via replica plating. Deletion of LANA was again verified by PCR, followed by sequencing of the PCR fragments, and the number of TRs was assessed by NheI digestion followed by pulsed-field gel electrophoresis (PFGE) (CHEF-DR II; Bio-Rad).

BAC LANA-R, BAC LANA-R Δ262–320, BAC LANA-R Δ288–320, BAC LANA-R Δ332–929, BAC LANA-R Δ465–929, and BAC LANA-R Δ331–495 were each obtained following recombination of transfer plasmid restriction fragments for each respective clone into BACΔLANA. To generate the WT LANA transfer plasmid, the kanamycin resistance gene from pEPCMV-in was amplified using primers 5′-ATA CGT *TGA TAT* CTA GGG ATA ACA GGG TAA TCG ATT TAT TC-3′ (EcoRV site in italics, kanamycin cassette sequence underscored) and 5′-GAT TAG G*TC TAG A*cg gtg gct tct agg gag gaa aaa ggg gga gag gtg tgg ct**T TTA TGT CAT TTC CTG TGG AGA GTC CCC AGG ACC TTG GTT** TGC TAG CCA GTG TTA CAA CCA ATT AAC C-3′ (XbaI site in italics, LANA sequence in bold, BAC16 sequence lowercase, kanamycin cassette sequence underscored). The resulting PCR product was cloned into pT7LANA following digestion with EcoRV and XbaI to generate the transfer plasmid containing the kanamycin expression cassette immediately downstream of LANA (*SI Appendix*, Fig. S1, *Right*).

To generate transfer plasmids for LANA mutants, XhoI/BamHI restriction fragments from pT7LANAΔ262–320, pT7LANAΔ288–320, pT7LANAΔ332–929, pT7LANAΔ465–929, or pT7LANAΔ331–495 were each introduced into the pT7LANA transfer plasmid following XhoI/BamHI digestion. (XhoI cuts just before the LANA ORF in pT7LANA, and BamH1 cuts at LANA codon 273.) Before recombination, all transfer plasmids were amplified in Dam-negative bacteria (to allow XbaI digestion) and digested with XhoI and XbaI, which

Downloaded at Universidade Católica Portuguesa on November 13, 2020

releases a fragment containing LANA and the downstream kanamycin cassette. The DNA fragments were recombined in BACΔLANA in a scarless fashion as described above.

The number of TR copies within each BAC clone was assessed by NheI digestion, followed by PFGE using 1% PFGE-grade agarose, at 5.5 V/cm for 16 h, an initial switch time of 1 s, and a final switch time of 5 s at 14 °C. NheI does not cut within the tandem TRs. KSHV contains approximately 40 TR copies of the 0.8-kb GC-rich TR element (27, 28). We observed that during BAC construction, the number of KSHV TRs was frequently reduced, presumably due to recombination events. Since LANA acts on the TRs to mediate episome persistence, and since TR copy number can affect LANA episome maintenance efficiency (29), we screened BAC recombinants with PFGE after NheI digestion to identify those with a full complement of TRs (*SI Appendix*, Fig. S2 *C* and *D*).

The recombinant BACs were confirmed for the ability to express GFP (BAC16 encodes a GFP expression cassette) following transfection into 293T cells (*SI Appendix*, Fig. S3). The recombinant BACs were also confirmed to be competent for the production of infectious KSHV following the induction of lytic replication, as described below (*SI Appendix*, Fig. S4).

pcDNA3 flag p53 encodes a 3× Flag epitope tag at the N terminus of p53. p53 containing substitution mutations was generated using reverse-orientation primers containing the mutated sequence to amplify the entire 3× Flag-p53 plasmid. The PCR amplification product was then incubated for 1 h with DpnI to digest template DNA and circularized using T4 ligase before transformation into *E. coli* bacteria. In brief, primer pairs P53-37023-RR: GGA***GCG***CAGGTGGCTGGAGTGAGCCCT and P53-37023-RF: ***CGCCGC***GGT CAGTCTACCTCCCGCCA (arginine codons in bold and italics) were used to amplify 3× Flag-p53 plasmid to mutate amino acids 370K, 372K, and 373K to arginines. The resulting mutant 3× Flag-p53 plasmid was then amplified by P53-38126-RR: GAG***GCGGCG***ATGGCGGGAGGTAGACTGAC and P53-38126-RF: ATGTTC***CGC***ACAGAAGGGCCTGACTCAG to mutate amino acids 381K, 382K, and 386K to arginines. Similarly, primers P53-37023-QR: GGA***CTG***CAG GTGGCTGGAGTGAGCCCT and P53-37023-QF: ***CAGCAG***GGTCAGTCTACCTCC CGCCA (glutamine codons in bold and italics) were used to amplify 3× Flag-P53 plasmid to mutate amino acids 370K, 372K, and 373K to glutamines. The resulting mutant 3× Flag-P53 plasmid was then amplified using P53-38126-QR: GAG***CTGCTG***ATGGCGGGAGGTAGACTGAC and P53-38126-QF: ATG TTC***CAG***ACAGAAGGGCCTGACTCAG to mutate amino acids 381K, 382K, and 386K to glutamines. All plasmids containing substitution mutations were sequence-confirmed.

pSP72 PCR 1_5 contains the kLANA ORF and its 5′ UTR (U75698; nts 123,808 to 127,886), flanked by MHV-68 DNA sequences (U97553; 104,710 to 105,092, upper flank; 102,728 to 103,934, lower flank) (30). pBamHI-G contains the MHV-68 BamHI G fragment (nts 101,653 to 106,902), which includes the mLANA ORF (nts 104,868 to 103,927) cloned into the BamHI site of the pST76K-SR (31) shuttle vector. DNA fragments comprising kLANA internal deletions were each subcloned into pSP72 PCR 1_5 from pT7 kLANAΔ332–929 and pT7 kLANAΔ465–929 (using BamHI/StuI). To create kLANA Δ331–495, the region between a PstI site in the 5′ UTR of kLANA (genomic nt 127,434) and codon 330 of kLANA was amplified with primers IMM AF3 (5′-GTA**CTGCAG**CCT GCTACTGTG-3′; 5′ UTR PstI site in bold) and IMM AF2 (5′-AAA**CTGCAG**ATCCTT ATTGTCATTGTCATC-3′; kLANA codon 330 underscored, introduced PstI site in bold) from pSP72_PCR1_4. pSP72_PCR1_4 is pSP72 PCR 1_5 without the lower MHV-68 flank (30). The PCR product was cloned into pSP72-PCR1_4 using PstI, replacing wild type by Δ331–495 kLANA sequences. The lower flank of MHV-68 was subcloned from pSP72-PCR1_5 into pSP72-PCR1_4 kLANA Δ331–495 using XhoI/HindIII. BglII-DNA fragments comprising mutant kLANA ORFs, the kLANA ORF 5′ UTR, and MHV-68 flanks were excised from each mutant pSP72-PCR1_5 and subcloned into the into BglII sites (MHV-68 genomic nts 102,728 and 105,087) of pBamHI-G. Mutant pBamHI-G shuttle vectors were recombined with wild-type MHV-68 BAC (pHA3) (31) or a yellow fluorescent protein (YFP) MHV-68 BAC (32) in *E. coli*. BAC recombinant clones were identified by colony PCR specific for kLANA and by analysis of EcoRI, BamHI, and HindIII restriction profiles of BAC DNA prepared from PCR-positive clones. Independent clones were generated for each virus.

Antibodies. KSHV LANA was detected using anti-LANA rat mAb (LN53) (13-210-100; ABI Sciences) and anti-LANA Ab (13). MHV68 LANA was detected with mAb 6A3 (30). Flag-p53 was detected using either anti-Flag M2 (Sigma-Aldrich) or p53 Ab (PA5-27822; Thermo Fisher Scientific). HA-CBP was detected using anti-CBP (A300-363A; Bethyl). GFP was detected with either mouse anti- GFP Ab (14-6674-82; Thermo Fisher Scientific) or rabbit anti-GFP (ab183734; Abcam). Actin was detected with an anti-actin rabbit polyclonal Ab (A2066; Sigma-Aldrich). Anti-CD19 APC-H7 (1D3) (557655; BD Biosciences), anti-GL-7 eF660 (GL7) (50-5902-82; eBioScience), and anti-CD95 PE (Jo2) (554258; BD Pharmingen) were used for FACS.

BAC Transfection, KSHV Production, and Infection. KSHV BAC DNA was purified from GS1783 *E. coli* cells using Midiprep kits (Macherey-Nagel). BACΔLANA, BACLANA-R, or BACLANA-R mutants were transfected into 293T cells with Lipofectamine 3000 (Thermo Fisher Scientific) following the manufacturer's protocol. Clonal selection was obtained using 0.2 mg/mL hygromycin (EMD Millipore). To assess the ability of the recombinant virus to produce virions, lytic reactivation was induced shortly after establishment of 293T stable cell lines containing BACΔLANA, BACLANA-R, or BACLANA-R LANA. Reactivation was induced overnight using TPA (20 ng/mL; Sigma-Aldrich) and sodium butyrate (32 mM; Alfa Aesar). At 5 d after reactivation, supernatant was harvested, filtered through a 0.45-μm filter (Celltreat), and used to infect 293T cells by spinoculation at 1,500 rpm for 1 h at room temperature. Cells were imaged using a Zeiss Axiovert microscope to assess for GFP expression from the recombinant BAC16.

LANA Expression Level. 293T cells were transfected with BACΔLANA, BACLANA-R, or BACLANA-R mutants and then harvested after 24 h. DNA was harvested from one-half of the cells using the Hirt extraction method (33). RNA was harvested from the other one-half of the cells by TRIzol (Life Technologies), following the manufacturer's protocol. RNAs were treated by RQ1 DNase (Promega) and then reverse-transcribed using the iScript Reverse Transcription Kit (Bio-Rad). Quantitative PCR (qPCR) was performed on DNA or cDNA using PowerUp CyberGreen Master Mix (Thermo Fisher Scientific) and LANA ORF73 primers 5′-GATGATTGTCCTGCGAAAGC-3′ and 5′- TTGGAT CTCGTCTTCCATCC-3′. The level of LANA cDNA was then divided by the level of LANA DNA (present in the virus genome) to determine LANA expression relative to the amount of virus DNA present for LANA or each LANA mutant.

LANA expression levels from infected BHK-21 cells were quantified by extracting cDNA (5 PFU/cell for 8 h) as described previously (34). Real-time qPCR was performed with the DyNAmo SYBR FlashGreen qPCR kit (Thermo Fisher Scientific), using primers specific for DNA encoding the C-terminal region of kLANA, (kLANA RT2-F: 5′-TGGTTGTTGGTATCTTGG-3′ and kLANA RT2-R: 5′-CCTGGAGTTCGTATGAGG-3′), and previously described primers for MHV68 M3 and for glyceraldehyde-3-phosphate dehydrogenase (34). ΔΔCT values (where CT is the threshold cycle) were calculated.

Colony Outgrowth Assays. BACΔLANA, BACLANA-R, or BACLANA-R mutants were transfected in 293T cells using Lipofectamine 3000. At 48 h after transfection, cells were assessed by flow cytometry for GFP expression (constitutively expressed from recombinant BAC16) and also counted manually. Total cell suspensions containing 1,000 GFP-expressing cells were plated in 15-cm dishes placed under 0.2 mg/mL hygromycin selection, for which resistance is encoded by BAC16. After 2.5 wk of selection, clones were stained with crystal violet and counted manually.

Western Blot and Immunoprecipitation Assays. Uninfected and infected (3 PFU/cell, 6 h) cell monolayers were washed three times with ice-cold PBS and scraped into lysis buffer (10 mM Tris·HCl pH 7.4, 150 mM NaCl, 1 mM NaF, 1 mM orthovanadate, 1% Triton X-100, and cOmplete Protease Inhibitor [Roche]). After a 20-min incubation on ice, samples were centrifuged at 18,000 × *g* for 10 min at 4 °C, and cleared lysates were analyzed by Western blot.

For immunoprecipitation experiments, 293T cells were transfected with the indicated plasmids using Lipofectamine 3000. Given our finding that CBP increases LANA expression and p53 decreases LANA or CBP expression, the amounts of transfected plasmids were adjusted to obtain similar LANA and p53 levels. Then 48 h later, cells were scraped into 1× PBS, and pellets were lysed in TNE buffer (100 mM Tris·HCl pH 8, 100 mM NaCl, 1 mM EDTA, and protease inhibitor [Thermo Fisher Scientific]) for 30 min on ice, followed by centrifugation for 10 min at 10,000 rpm. Then 20 μL of Dynabeads Protein G (Invitrogen) was incubated with 4 μg of M2-Flag Ab (Sigma-Aldrich) in TNE buffer for 2 h at 4 °C, followed by two washings with TNE buffer. The Ab-bound Dynabeads were incubated with cell lysate supernatant overnight at 4 °C with 2,000 U/mL micrococcal nuclease and 10 mM $CaCl_2$ included in the incubation. Beads were washed five times in IPP50 buffer (10 mM Tris·HCl pH 8, 150 mM NaCl, and 1% Triton X-100) with protease inhibitor and then boiled for 10 min.

For immunoprecipitations with p53 mutants, 5 μg of plasmid encoding GFP-LANA or GFP-LANA 275–435 was cotransfected with 5 μg of plasmid encoding 3FLAG-p53, 3FLAG-p53 KR, or 3Flag-p53 KQ into cells in 10-cm dishes containing 293T cells at 70% confluence using lipofectamine 3000 regent (Thermo Fisher Scientific). After incubation at 37 °C for 48 h, cells

Downloaded at Universidade Católica Portuguesa on November 13, 2020

were lysed in lysis buffer (20 mM Tris pH 7.9, 137 mM NaCl, 1% Triton X-100, 10 mM $CaCl_2$, 2 mM EDTA, 10% glycerol, and 2000 U/mL micrococcal nuclease) and subjected to centrifugation to obtain cell lysate supernatant. Dynabeads Protein G (Invitrogen) were incubated with mouse anti-Flag monoclonal Ab (Sigma-Aldrich; 1804) in lysis buffer for 30 min at 37 °C and then washed three times with lysis buffer. The Flag Ab-bound Dynabeads were then incubated with cell lysate supernatant overnight at 4 °C. Input (5%) and immunoprecipitates were analyzed by Western blot analysis with rabbit monoclonal anti-GFP (Abcam; 183734) to detect GFP-LANA or GFP-LANA 275–435 or with mouse anti-Flag (Sigma-Aldrich; 1804) to detect 3FLAG-P53. Images were captured and quantitation performed using the LI-COR Odyssey imaging system.

Virus Reconstitution and Stocks. Here 1 μg of each recombinant MHV-68 BAC DNA (Maxiprep DNA; Macherey-Nagel) was used to transfect 10^6 BHK-21 cells in a 6 cm diameter dish with X-tremeGENE HP (GE Healthcare). About 4 d after transfection, when CPE was visible, cells and media were harvested and frozen-thawed. Viruses were passaged through NIH 3T3-CRE cells to remove loxP-flanked BAC sequences. Loss of green fluorescence in viral plaques was indicative of removal of BAC DNA, which expresses the GFP.

MHV-68 (v-WT) and v-WT.yfp virions were reconstituted from BAC DNA. v-kLANA and v-kLANA.yfp have been described previously (30). Virus stocks were prepared by infecting BHK-21 cells at 0.002 PFU/cell for 3 to 5 d. Medium from infected cultures was harvested and cleared by centrifugation at 500 × *g* for 5 min at 4 °C. Viruses were recovered from cleared supernatants by centrifugation at 15,000 × *g* for 2 h at 4 °C.

Mice. Female C57BL/6J mice were purchased from Charles River Laboratories and housed and subjected to experimental procedures in specific pathogen-free conditions at Instituto de Medicina Molecular (IMM). All experiments were approved by the Direção-Geral de Alimentação e Veterinária (protocol AEC_2010_017_PS_Rdt_General) and the IMM Animal Ethics Committee.

Infectivity Assays. Virus titration was performed in BHK-21 cells by suspension assay (plaque assay). After a 4-d incubation at 37 °C, cells were fixed with 4% formaldehyde in PBS and stained with 0.05% toluidine blue. Viral plaques were counted manually under a plate microscope. Female C57 BL6 J mice (age 6 to 8 wk) were infected intranasally with 10^4 PFU in 20 μL of PBS under isofluorane anesthesia. Single-cell suspensions of spleens were prepared as described previously (34). For the infectious center assay (ex vivo reactivation assay), serially diluted splenocyte suspensions from individual mice were cocultured with 5×10^5 BHK-21 cells in 6-cm dishes for 5 d at 37 °C. Cells were fixed and stained and viral plaques were counted manually, as for the plaque assay. Preformed infectious virus titers in freeze-thawed splenocyte suspensions were determined by a plaque assay. The frequency of viral genome-positive cells was determined by limiting dilution combined with PCR detection of viral genomes (35, 36). Pools from individual splenocyte suspensions (starting at 2×10^6 cells) or FACS-sorted germinal center B cells ($CD19^+CD95^+GL7^+$) (30) were twofold serially diluted. Eight replicates for each dilution were incubated with lysis buffer (10 mM Tris·HCl pH 8.3, 3 mM $MgCl_2$, 50 mM KCl, 0.45% Nonidet P-40, 0.45% Tween 20, and 0.5 mg/mL of proteinase K), overnight at 37 °C and, after Proteinase K inactivation (95 °C for 5 min), subjected to real-time qPCR. MHV-68 M9 gene-specific primers and TaqMan probe and PCR settings have been described previously (35). Positive and negative reactions were scored using Rotor Gene 6000 software. The frequency of viral DNA^+ cells was determined by regression analysis of the number of cells vs. the fraction of PCR-negative results.

Results

LANA Residues 332 to 465 Mediate Latent KSHV Infection. We previously identified internal LANA sequence as critical for LANA-mediated episome persistence. While N- and C-terminal LANA are essential for episome persistence, deletion of internal LANA regions induce a broad range of deficiencies, ranging from mild to severe. These deficiencies were characterized using an episome

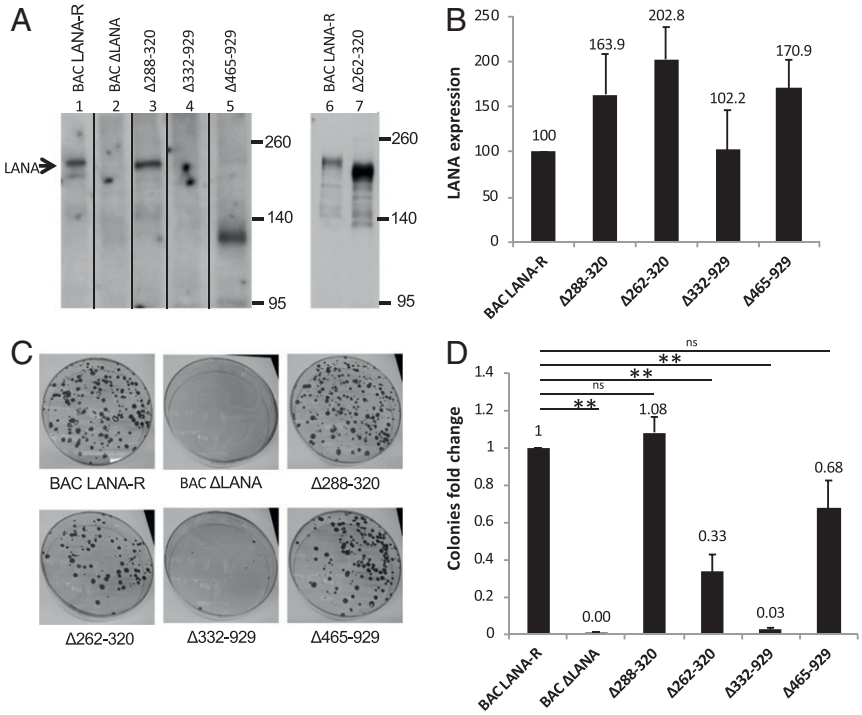

Fig. 2. BAC LANA-R Δ332–929 is abolished, and BAC LANA-R Δ262–320 is impaired for latently infected cell outgrowth. (*A*) BACΔLANA, BAC LANA-R, and BAC containing LANA mutants were transfected into 293T cells. The cells were harvested after 48 h, and LANA expression was assessed by Western blot analysis using a polyclonal Ab that recognizes the LANA internal repeat elements. (*B*) BACΔLANA, BAC LANA-R, and LANA mutants were each transfected into 293T cells and harvested after 24 h. DNA was extracted by Hirt extraction (33). RNA was extracted with TRIzol and reverse-transcribed. The level of LANA cDNA compared with KSHV DNA, as determined by real-time qPCR, was used to determine expression levels. (*C* and *D*) BAC LANA-R and mutants were transfected in 293T cells. At 48 h posttransfection, the number of GFP-expressing cells (i.e., GFP expressed from the recombinant BAC) was assessed by flow cytometry, and a cell suspension containing 1,000 green cells was plated and placed under selection, for which resistance is encoded by the BAC, in 150-mm dishes. After 2.5 wk of selection, colonies were stained with crystal violet and counted. A representative experiment is shown in *C*, and average colony outgrowths are shown in *D*. All data are from at least three independent experiments. ns, $P > 0.05$. $^{**}P < 0.01$, independent-samples *t* test.

Downloaded at Universidade Católica Portuguesa on November 13, 2020

maintenance assay in which LANA mediates episome persistence of TR DNA. This assay has a broad dynamic range, allowing for detection of LANA deficiencies ranging up to several thousand-fold (13, 14, 37–39).

Since previous assays were performed in the absence of other KSHV genes, we wished to assess the role of mild or modest LANA deficiencies for virus persistence. It is possible that comparatively "mild" deficiencies in LANA function could exert a substantial effect on the ability of KSHV to persist; for instance, compensatory recombination events that are selected for in TR episomes in the absence of other virus genes would likely induce lethal events for virus. Disruption of virus persistence due to deletion of specific LANA sequences would indicate a critical biological function.

We generated recombinant KSHV BAC16 (24) containing WT LANA (BAC LANA-R), KSHV lacking LANA (BACΔLANA), and KSHV containing LANAΔ288–320 (BAC LANA-R Δ288–320), LANAΔ262–320 (BAC LANA-R Δ262–320), LANAΔ465–929 (BAC LANA-R Δ465–929), or LANAΔ332–929 (BAC LANA-R Δ332–929) (Fig. 1). LANAΔ288–320, LANAΔ262–320, LANAΔ465–929, and LANAΔ332–929 have mild or modest episome maintenance deficiencies of 3.0-, 14.4-, 3.8-, and 10.9-fold, respectively, which contrast sharply with deficiencies of at least several hundred-fold after deletion of distinct LANA sequences (13, 38). LANAΔ262–320 is deficient since it lacks interaction with the DNA replication factor C (RFC), engendering a deficiency for LANA-mediated DNA replication, while LANAΔ288–320 retains RFC interaction (14, 40).

Since LANA can regulate its own expression (41), LANA expression was assessed from the recombinant LANA mutant BACs. Following BAC transfection into 293T cells, LANA, LANAΔ288–320, LANAΔ465–929, and LANAΔ262–320 could each be detected by immunoblot migration at the appropriate size (Fig. 2*A*). As expected, LANAΔ332–929, which lacks the internal repeats to which most anti- LANA Abs are directed, was not detected by immunoblot. Direct comparison of LANA expression through assessment of LANA transcript levels demonstrated each of the LANA mutants was expressed at a level at least as high as that of WT (Fig. 2*B*).

We assessed the recombinant KSHVs for the ability to establish latency and persist in cells. BACΔLANA, BAC LANA-R, or BAC containing LANAΔ288–320, LANAΔ262–320, LANAΔ465–929, or LANAΔ332–929 was transfected into 293T cells. At 48 h post-transfection, 1,000 virus-infected cells, as assessed by GFP expression from the recombinant viral genome, were seeded into 15-cm dishes and placed under hygromycin selection, for which the recombinant genome encodes resistance. After 2.5 wk of selection, the number of hygromycin-resistant 293T cell colonies was determined (Fig. 2 *C* and *D*). As expected, BAC LANA-R resulted in efficient outgrowth, while BACΔLANA, which lacks LANA and thus cannot establish persistent latent infection, was abolished for outgrowth. BAC LANA-R Δ288–320 persisted similarly to BAC LANA-R, while BAC LANA-R Δ262–320 persisted at only 33% of the WT BAC LANA-R levels. BAC LANA-R Δ465–929, which lacks most of the LANA internal repeat elements, was reduced only modestly and persisted at ∼70% of WT levels. In stark contrast, BAC LANA-R Δ332–929, which lacks all LANA internal repeat elements, lost the ability to persist.

Since the only difference between LANAΔ465–929 and LANAΔ332–929 is deletion of residues 332 to 465, we directly tested the role of these LANA residues by deleting them in BAC LANA-R Δ331–495. Following transfection of BAC LANA-R Δ331–495 into 293T cells, LANA Δ331–495 was detected by immunoblot migration at the appropriate size (Fig. 3*A*). Compared with BAC LANA-R, BAC LANAΔ331–495 had highly deficient outgrowth, at 25% of the level in WT BAC LANA-R (Fig. 3 *B* and *C*). Taken together, these data indicate that LANA residues 332 to 465 are necessary for the efficient establishment of KSHV latency and persistence in cells.

LANA 332–465 Contains an Acidic Domain Reader Sequence That Selectively Interacts with Nonacetylated p53. Within LANA residues 332 to 465, we identified amino acids 330 to 421 as having high homology with the SET oncoprotein acidic domain reader region (Fig. 4*A*). The SET reader region preferentially interacts with unacetylated forms of lysine-rich ligands, including the carboxy terminal domain of p53 (23). Alignment of the SET acidic region with LANA reveals two overlapping regions of homology between LANA amino acids 330 and 421, which encompasses almost all of the LANA 332 to 465 sequence necessary for efficient virus persistence (Fig. 4*A*). A lower homology match is also present in C-terminal LANA residues 845 to 895.

Since LANA interacts with p53 (42–44), we assessed the interaction between the LANA acidic domain region and p53. GFP LANA 275–435, which contains the acidic sequence, coimmunoprecipitated with p53 with similar efficiency as that of GFP LANA (Fig. 4*B*), indicating that this LANA region interacts with p53. Since CBP acetylates p53, we evaluated the interaction of LANA in the presence or absence of CBP overexpression. As expected, LANA coimmunoprecipitated with p53 (Fig. 4*C*, lane 5); however, in the presence of CBP expression, LANA's interaction with p53 was substantially diminished (Fig. 4*C*, lane 6), consistent with p53 acetylation reducing the

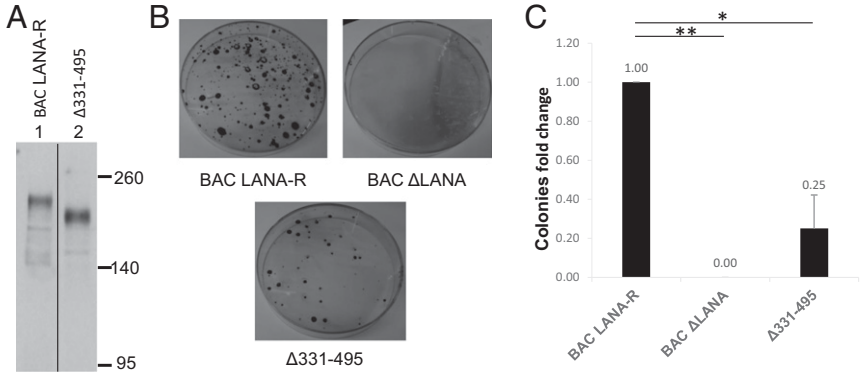

Fig. 3. BAC LANA-R Δ331–495 is severely impaired for latently infected cell outgrowth. (*A*) BAC LANA-R and BAC LANA-R Δ331–495 were transfected into 293T cells. The cells were harvested after 48 h, and LANA expression was assessed by Western blot analysis. (*B* and *C*) BAC LANA-R and BAC LANA-R Δ331–495 were each transfected into 293T cells. At 48 h after transfection, the cells were plated and placed under selection as described in Fig. 2. Data in *C* are from at least three independent experiments. $*P < 0.05$; $**P < 0.01$.

Downloaded at Universidade Católica Portuguesa on November 13, 2020

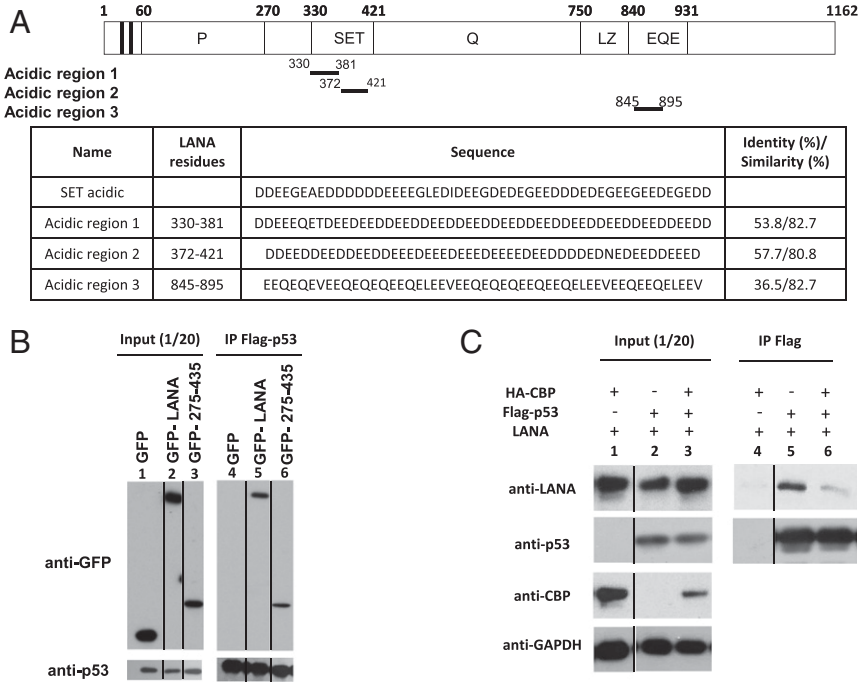

Name	LANA residues	Sequence	Identity (%)/ Similarity (%)
SET acidic		DDEEGEAEDDDDDDEEEEGLEDIDEEGDEDEGEEDDDEDEGEEGEEDEGEDD	
Acidic region 1	330-381	DDEEEQETDEEDEEDDEEDDEEDDEEDDEEDDEEDDEEDDEEDDEEDDEEDD	53.8/82.7
Acidic region 2	372-421	DDEEDDEEDDEEDDEEEDEEEDEEEDEEEEDEEDDDDEDNEDEEDDEEED	57.7/80.8
Acidic region 3	845-895	EEQEQEVEEQEQEQEEQELEEVEEQEQEQEEQEELEEVEEQEEQELEEV	36.5/82.7

Fig. 4. The LANA SET homology sequence interacts with p53 and acetylation reduces LANA–p53 interaction. (*A*) Schematic of LANA with acidic SET homology regions indicated below. Sequence alignments were determined with LALIGN. Identity and similarity are shown. (*B*) GFP LANA 275–435 interacts with p53. GFP, GFP-LANA, or GFP-LANA 275–435 and Flag-p53 were cotransfected into 293T cells. At 48 h after transfection, Flag p53 was immunoprecipitated with M2-Flag Ab, and Western blot analysis was performed. (*C*) Expression of CBP, which acetylates p53, reduces the LANA–p53 interaction. pT7LANA, Flag-p53, and HA-CBP were transfected into 293T cells. At 48 h after transfection, Flag p53 was immunoprecipitated using M2-Flag Ab, and Western blot analysis was performed. Data in *B* and *C* are representative of at least three independent experiments.

interaction. Since CBP functionally interacts with LANA and p53 (45, 46), we also examined LANA's p53 binding in the absence of CBP overexpression.

We assessed LANA binding to an acetylation mimicking carboxy terminal domain p53 mutant, $p53^{KQ}$, or to an acetylation-deficient mutant, $p53^{KR}$ (23). After expression in 293T cells, LANA coprecipitated with $p53^{KR}$ more efficiently than with WT p53 (Fig. 5*A*). In direct contrast, LANA's interaction with acetylation mimicking $p53^{KQ}$ was substantially reduced (Fig. 5*A*). Furthermore, GFP LANA 275–435 demonstrated a similar pattern of interaction with enhanced binding to $p53^{KR}$ and reduced binding to $p53^{KQ}$ (Fig. 5*B*). Taken together, these results indicate that the LANA acidic domain preferentially interacts with unacetylated p53.

The LANA Acidic Domain Reader Is Required for Latency of Chimeric MHV-68 in Vivo. We next interrogated the function of the acidic domain reader of LANA in a more physiological setting. We and others have previously described a v-kLANA chimeric virus in which MHV-68 LANA is replaced by KSHV LANA in MHV-68 as a model system for investigating LANA function during in vivo infection of mice (30, 47). KSHV LANA rescued the ability of the chimeric virus to establish latent infection in vivo, although at a moderately reduced level compared with wild-type MHV-68. As expected, mutations in the essential LANA histone-binding region or DNA-binding domain abolished the latency of the chimeric virus (30). To assess the contribution of the internal repeat regions of LANA to v-kLANA latency, we generated recombinant chimeric viruses containing LANA Δ332–929 and Δ465–929. Transcripts of LANA Δ465–929 and Δ332–929 were detected following infection of BHK-21 cells with each mutant virus (Fig. 6*A*). Both mutant viruses underwent lytic replication normally in vitro (Fig. 6*B*).

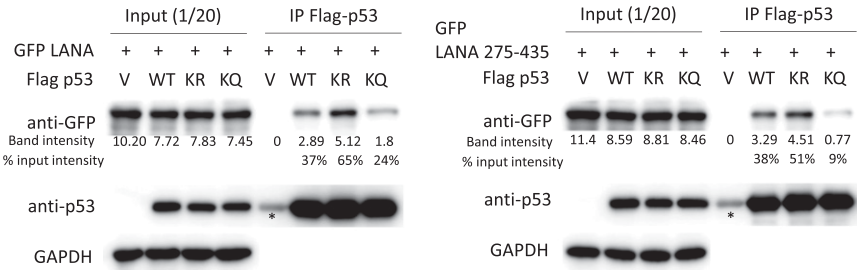

Fig. 5. Decreased LANA interaction with acetylation mimicking $p53^{KQ}$ and increased LANA interaction with acetylation-deficient $p53^{KR}$. GFP LANA (*Left*) and GFP LANA 275–435 (*Right*) were coexpressed with Flag p53, $p53^{KQ}$, or $p53^{KR}$ (p53 K acetylation sites 370, 372 to 373, 381 to 382, and 386 mutated to Q or R, respectively) in 293T cells. At 48 h posttransfection, Flag p53 was immunoprecipitated, and Western blot analysis was performed. Results are representative of at least three experiments. Quantitation of GFP LANA or GFP LANA 275–435 bands are shown. *Heavy chain, which comigrates with p53. V, Flag vector.

Downloaded at Universidade Católica Portuguesa on November 13, 2020

We next inoculated mice intranasally and assessed viral latency in the spleen at day 14 postinoculation, at the peak of expansion of latently infected cells at this dose and route of infection. Latent virus load was assessed by an ex vivo reactivation/infectious assay that measures reactivating virus from total splenocytes on coculture with permissive fibroblasts, and by limiting dilution analysis with PCR detection of viral DNA-positive cells to determine the frequency of infection. v-Δ332–929 was undetectable in both assays (Fig. 6 *C* and *D* and *SI Appendix*, Table S1). In contrast, v-Δ465–929 latency was indistinguishable from that of v-kLANA (Fig. 6 *C* and *D* and *SI Appendix*, Table S1).

We next constructed a chimeric MHV-68 containing LANA Δ331–495. The LANA Δ331–495 protein was expressed in infected cells in vitro, migrating at appropriate size and with similar levels as wild-type protein (Fig. 7*A*). v-Δ331–495 had similar growth in vitro as v-kLANA and v-WT viruses (Fig. 7*B*). On inoculation of mice, at 14 d after infection, v-Δ331–495 was deficient for latency establishment compared with v-kLANA, with undetectable virus in most mice and low levels in the remaining mice in ex vivo reactivation/infectious titers (Fig. 7 *C* and *D*, *Left*). In agreement with these results, the frequency of infection in total splenocytes was roughly 10-fold lower for v-Δ331–495 compared with v-kLANA (Fig. 7*D*, *Right* and *SI Appendix*, Table S2). Therefore, LANA residues 332 to 465 of the internal repeat region that contains the acidic domain reader are critical not only for efficient KSHV latency establishment, but also for chimeric virus latency in vivo.

Discussion

This work shows that LANA residues 330 to 421 contain an SET homologous acidic domain reader sequence that preferentially interacts with the unacetylated form of p53. Such a "reader" sequence is functionally opposite of bromodomains, which bind acetylated ligands (48). This LANA sequence may exert its effects on viral persistence through p53. LANA inhibits p53 activity (42), and interaction with the unacetylated form of p53 could contribute to this inhibition. However, it is likely that LANA also preferentially interacts with unacetylated forms of additional proteins. The species-specific prediction of lysine acetylation (SSPKA) program (49) identifies 49 host proteins other than p53 that contain lysine clusters with the potential to selectively bind acidic domain readers in an unacetylated form (23). Many of these proteins have been described as potential LANA-interacting partners (46, 50–55), and LANA may exert its effects on virus persistence through one or more of these. For instance, LANA interacts with the cAMP response element-binding protein (CBP) and inhibits its acetylase and transcriptional activity (46). Two LANA regions, C-terminal LANA and the acidic domain reader sequence, interact with the CBP C/H3 region, and this region contains lysine residues that are predicted to be acetylated (23).

LANA contains two tandem, partially overlapping acidic domain reader sequences between residues 330 and 421 and a third, lower-homology C-terminal acidic domain reader sequence at amino acids 845 to 895 (Fig. 4). In contrast, 49 host proteins identified as containing potential acidic domain reader sequences generally contain less extensive acidic sequences of approximately one-half the length of LANA 330 to 421 (23). The basis for LANA's extended acidic domain reader sequence is unclear. Perhaps LANA acts as a multivalent receptor for one or more unacetylated partners. Such interactions could be inhibitory, similar to that of SET on p53, or could assemble active complexes important for virus persistence.

LANA inhibits *cis* major histocompatibility complex (MHC) class I antigen presentation, with the LANA central repeat elements

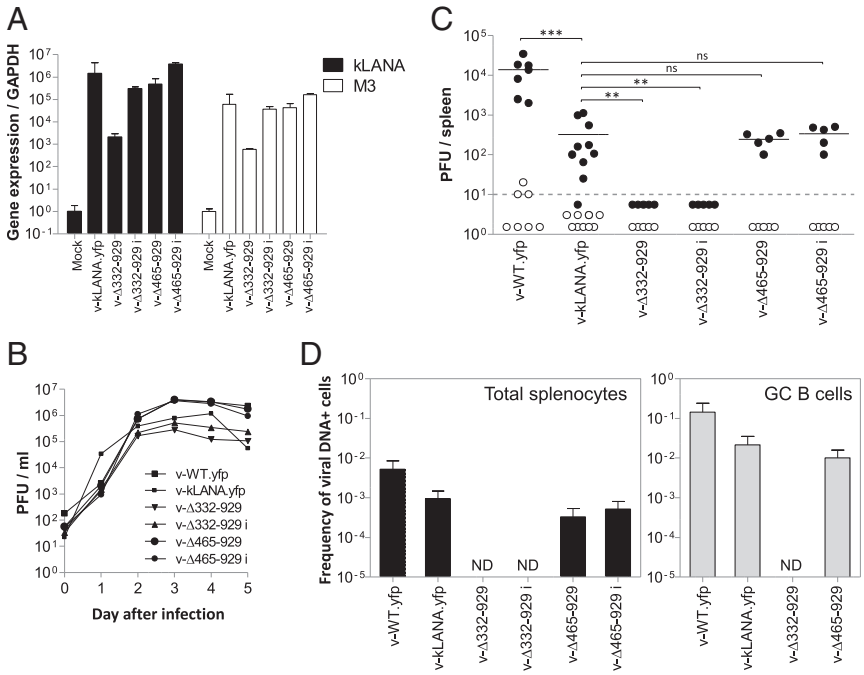

Fig. 6. Deletion of kLANA residues 332 to 929 abolishes kLANA-MHV-68 latency in vivo. (*A*) Relative levels of kLANA transcripts from BHK-21 cells infected with 5 PFU/cell for 8 h. Expression of MHV68 M3, a lytic viral product, was also assessed as a measure of the level of infection. Bars indicate mean fold changes ± SD. (*B*) Growth curves. BHK-21 cells were infected with 0.01 PFU/cell for 1 h and, after removal of inoculum and washing, incubated at 37 °C. Total virus titers at the indicated times were determined by plaque assay. Time 0 represents the viral titer after washing inoculum. (*C* and *D*) Latent infection in the spleen at day 14 after intranasal infection with 10^4 PFU. (*C*) Infectious center titers following reactivation from latency (closed circles) and preformed virus (open circles). Circles represent individual mice. The horizontal bar indicates the mean, and the dashed line indicates the limit of detection. (*D*) Frequency of viral DNA-positive cells (bars) ± 95% CIs in total splenocytes (*Left*) and FACS-sorted germinal center B cells ($CD19^+CD95^+GL7^+$) (*Right*). Data are from pools of three to five spleens per infection group. ND, not detectable. i denotes independent clone. NS, not significant; $^{**}P < 0.01$; $^{***}P < 0.001$, Mann–Whitney *U* test.

Downloaded at Universidade Católica Portuguesa on November 13, 2020

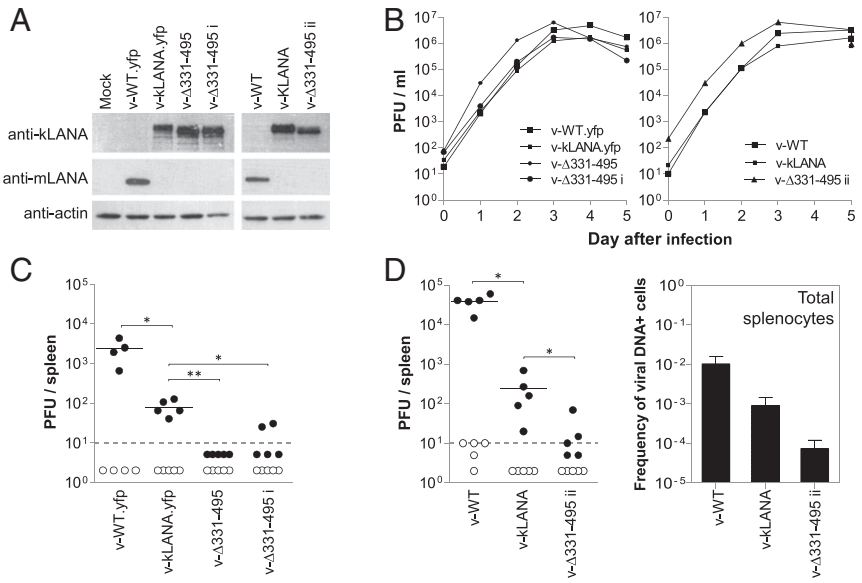

Fig. 7. LANA residues 331 to 495 are required for efficient establishment of viral latency in infected mice. (*A*) Detection of kLANA Δ331–495 by Western blot in infected BHK-21 cells (3 PFU/cell; 6 h postinfection), using an Ab specific for the repeat region. mLANA was detected specifically in v-WT–infected cells. Anti-actin immunoblots confirmed equivalent amounts of cellular extracts among the samples. (*B*) Growth curves in BHK-21 cells following infection with 0.01 PFU/cell performed as in Fig. 6*B*. (*C* and *D*) Latent infection in the spleen at 14 d after intranasal infection with 10^4 PFU. (*C* and *D*, *Left*), Infectious center titers (closed circles) and preformed virus (open circles). Circles represent individual mice. The horizontal bar indicates the mean, and the dashed line represents the limit of detection. (*D*, *Right*) Frequency of viral DNA-positive cells (bars) ± 95% CIs in total splenocytes. Data are from pools of five spleens per infection group. i and ii denote independent clones.*$P < 0.05$; **$P < 0.01$, Mann–Whitney *U* test.

responsible for this function (56–58). The glutamine-rich repeat sequence retards LANA synthesis, which is expected to reduce defective ribosomal product processing, and also enhances the stability of LANA. EBNA1, LANA's functional episome maintenance homolog in the Epstein–Barr virus, exhibits similar properties, which result in inhibition of antigen presentation by MHC class I molecules (59, 60). However, despite these functions, deletion of the glutamine-rich region did not reduce LANA's ability to inhibit *cis* MHC class I peptide presentation (57) or virus persistence in the experiments presented here. The LANA acidic domain does not affect LANA synthesis or stability, but it does inhibit *cis* MHC class I peptide presentation (57). The mechanism for this inhibition is unknown, and it is intriguing to consider that LANA may exert this effect through acidic domain interaction with an unacetylated partner. Although the loss of such inhibition in the absence of the acidic domain could contribute to a loss of virus persistence in vivo, it would not account for the observed loss of KSHV persistence in cell culture, suggesting that additional factors are responsible.

In contrast to KSHV LANA, MHV68 LANA lacks repeat elements, including an acidic domain reader sequence. Since the MHV68 LANA DNA-binding domain multimerizes into higher-order structures and recognizes DNA differently from KSHV LANA (61), it is possible that the acidic domain reader sequence has evolved in concert with differences in LANA's recognition of DNA. For instance, if the bend in DNA induced by KSHV LANA signals a DNA damage response, similar to that triggered by bends due to insertion/deletion loops (62, 63), such a response could be countered by a recruited factor. In contrast, MHV68 LANA does not induce a bend in DNA and would not require such an interaction.

In summary, here we have shown that LANA contains an acidic domain reader, homologous to the SET acidic domain, that recognizes the unacetylated form of tumor suppressor p53. Like SET, the LANA acidic domain may function as a transcriptional corepressor of p53. However, LANA's acidic domain reader could potentially interact with other cellular partners that have a lysine cluster to exert its functional effects. Disrupting the key interaction(s) through which the LANA acidic domain exerts its effects may offer the opportunity for the development of strategies to prevent or treat persistent KSHV infection and associated tumors.

Data Availability. All study data are included in the main text and *SI Appendix*.

ACKNOWLEDGMENTS. We thank Kevin Brulois for advice on cloning BAC LANA-R, Ana P. Quendera for technical help, and staff at the rodent facility at IMM for support. This work was supported by NIH grants CA082036, DE025208, AI150575, and DE024971 (to K.M.K.); Fondation ARC pour la recherche sur le cancer Grant SAE20121206018 (to F.J.); and Fundação para a Ciência e Tecnologia Grant PTDC/IMI-MIC/0980/2014 (to J.P.S.).

1. S. M. Reed, D. E. Quelle, p53 acetylation: Regulation and consequences. *Cancers (Basel)* **7**, 30–69 (2014).
2. P. Filippakopoulos *et al*., Histone recognition and large-scale structural analysis of the human bromodomain family. *Cell* **149**, 214–231 (2012).
3. D. Wang, N. Kon, O. Tavana, W. Gu, The "readers" of unacetylated p53 represent a new class of acidic domain proteins. *Nucleus* **8**, 360–369 (2017).
4. Y. Chang *et al*., Identification of herpesvirus-like DNA sequences in AIDS-associated Kaposi's sarcoma. *Science* **266**, 1865–1869 (1994).
5. E. Cesarman, Y. Chang, P. S. Moore, J. W. Said, D. M. Knowles, Kaposi's sarcoma-associated herpesvirus-like DNA sequences in AIDS-related body-cavity-based lymphomas. *N. Engl. J. Med.* **332**, 1186–1191 (1995).
6. P. S. Moore, Y. Chang, Detection of herpesvirus-like DNA sequences in Kaposi's sarcoma in patients with and those without HIV infection. *N. Engl. J. Med.* **332**, 1181–1185 (1995).
7. J. Soulier *et al*., Kaposi's sarcoma-associated herpesvirus-like DNA sequences in multicentric Castleman's disease. *Blood* **86**, 1276–1280 (1995).
8. M. E. Ballestas, K. M. Kaye, The latency-associated nuclear antigen, a multifunctional protein central to Kaposi's sarcoma-associated herpesvirus latency. *Future Microbiol.* **6**, 1399–1413 (2011).
9. L. Cherezova, K. L. Burnside, T. M. Rose, Conservation of complex nuclear localization signals utilizing classical and non-classical nuclear import pathways in LANA homologs of KSHV and RFHV. *PLoS One* **6**, e18920 (2011).

Downloaded at Universidade Católica Portuguesa on November 13, 2020

10. T. Piolot, M. Tramier, M. Coppey, J. C. Nicolas, V. Marechal, Close but distinct regions of human herpesvirus 8 latency-associated nuclear antigen 1 are responsible for nuclear targeting and binding to human mitotic chromosomes. *J. Virol.* **75**, 3948–3959 (2001).
11. A. J. Barbera *et al*., The nucleosomal surface as a docking station for Kaposi's sarcoma herpesvirus LANA. *Science* **311**, 856–861 (2006).
12. A. J. Barbera, M. E. Ballestas, K. M. Kaye, The Kaposi's sarcoma-associated herpesvirus latency-associated nuclear antigen 1 N terminus is essential for chromosome association, DNA replication, and episome persistence. *J. Virol.* **78**, 294–301 (2004).
13. E. De Leon Vazquez, V. J. Carey, K. M. Kaye, Identification of Kaposi's sarcoma-associated herpesvirus LANA regions important for episome segregation, replication, and persistence. *J. Virol.* **87**, 12270–12283 (2013).
14. E. De León Vázquez, F. Juillard, B. Rosner, K. M. Kaye, A short sequence immediately upstream of the internal repeat elements is critical for KSHV LANA-mediated DNA replication and impacts episome persistence. *Virology* **448**, 344–355 (2014).
15. M. E. Ballestas, P. A. Chatis, K. M. Kaye, Efficient persistence of extrachromosomal KSHV DNA mediated by latency-associated nuclear antigen. *Science* **284**, 641–644 (1999).
16. A. C. Garber, J. Hu, R. Renne, Latency-associated nuclear antigen (LANA) cooperatively binds to two sites within the terminal repeat, and both sites contribute to the ability of LANA to suppress transcription and to facilitate DNA replication. *J. Biol. Chem.* **277**, 27401–27411 (2002).
17. M. E. Ballestas, K. M. Kaye, Kaposi's sarcoma-associated herpesvirus latency-associated nuclear antigen 1 mediates episome persistence through cis-acting terminal repeat (TR) sequence and specifically binds TR DNA. *J. Virol.* **75**, 3250–3258 (2001).
18. M. A. Cotter 2nd, E. S. Robertson, The latency-associated nuclear antigen tethers the Kaposi's sarcoma-associated herpesvirus genome to host chromosomes in body cavity-based lymphoma cells. *Virology* **264**, 254–264 (1999).
19. L. Rodrigues *et al*., Termination of NF-kappaB activity through a gammaherpesvirus protein that assembles an EC5S ubiquitin-ligase. *EMBO J.* **28**, 1283–1295 (2009).
20. X. Li, D. Liang, X. Lin, E. S. Robertson, K. Lan, Kaposi's sarcoma-associated herpesvirus-encoded latency-associated nuclear antigen reduces interleukin-8 expression in endothelial cells and impairs neutrophil chemotaxis by degrading nuclear p65. *J. Virol.* **85**, 8606–8615 (2011).
21. L. Rodrigues, N. Popov, K. M. Kaye, J. P. Simas, Stabilization of Myc through heterotypic poly-ubiquitination by mLANA is critical for γ-herpesvirus lymphoproliferation. *PLoS Pathog.* **9**, e1003554 (2013).
22. P. G. Stevenson *et al*., K3-mediated evasion of CD8(+) T cells aids amplification of a latent gamma-herpesvirus. *Nat. Immunol.* **3**, 733–740 (2002).
23. D. Wang *et al*., Acetylation-regulated interaction between p53 and SET reveals a widespread regulatory mode. *Nature* **538**, 118–122 (2016).
24. K. F. Brulois *et al*., Construction and manipulation of a new Kaposi's sarcoma-associated herpesvirus bacterial artificial chromosome clone. *J. Virol.* **86**, 9708–9720 (2012).
25. O. Gjoerup, D. Zaveri, T. M. Roberts, Induction of p53-independent apoptosis by simian virus 40 small t antigen. *J. Virol.* **75**, 9142–9155 (2001).
26. B. Kelley-Clarke, M. E. Ballestas, T. Komatsu, K. M. Kaye, Kaposi's sarcoma herpesvirus C-terminal LANA concentrates at pericentromeric and peri-telomeric regions of a subset of mitotic chromosomes. *Virology* **357**, 149–157 (2007).
27. M. Lagunoff, D. Ganem, The structure and coding organization of the genomic termini of Kaposi's sarcoma-associated herpesvirus. *Virology* **236**, 147–154 (1997).
28. J. G. Judde *et al*., Monoclonality or oligoclonality of human herpesvirus 8 terminal repeat sequences in Kaposi's sarcoma and other diseases. *J. Natl. Cancer Inst.* **92**, 729–736 (2000).
29. P. Shrestha, B. Sugden, Identification of properties of the Kaposi's sarcoma-associated herpesvirus latent origin of replication that are essential for the efficient establishment and maintenance of intact plasmids. *J. Virol.* **88**, 8490–8503 (2014).
30. A. C. Habison *et al*., Cross-species conservation of episome maintenance provides a basis for in vivo investigation of Kaposi's sarcoma herpesvirus LANA. *PLoS Pathog.* **13**, e1006555 (2017).
31. H. Adler, M. Messerle, M. Wagner, U. H. Koszinowski, Cloning and mutagenesis of the murine gammaherpesvirus 68 genome as an infectious bacterial artificial chromosome. *J. Virol.* **74**, 6964–6974 (2000).
32. C. M. Collins, J. M. Boss, S. H. Speck, Identification of infected B-cell populations by using a recombinant murine gammaherpesvirus 68 expressing a fluorescent protein. *J. Virol.* **83**, 6484–6493 (2009).
33. B. Hirt, Selective extraction of polyoma DNA from infected mouse cell cultures. *J. Mol. Biol.* **26**, 365–369 (1967).
34. M. Pires de Miranda, A. P. Quendera, C. E. McVey, K. M. Kaye, J. P. Simas, In vivo persistence of chimeric virus after substitution of the Kaposi's sarcoma-associated herpesvirus LANA DNA binding domain with that of Murid herpesvirus 4. *J. Virol.* **92**, e01251-18 (2018).
35. J. Decalf, C. Godinho-Silva, D. Fontinha, S. Marques, J. P. Simas, Establishment of murine gammaherpesvirus latency in B cells is not a stochastic event. *PLoS Pathog.* **10**, e1004269 (2014).
36. S. Marques, S. Efstathiou, K. G. Smith, M. Haury, J. P. Simas, Selective gene expression of latent murine gammaherpesvirus 68 in B lymphocytes. *J. Virol.* **77**, 7308–7318 (2003).
37. B. Kelley-Clarke, E. De Leon-Vazquez, K. Slain, A. J. Barbera, K. M. Kaye, Role of Kaposi's sarcoma-associated herpesvirus C-terminal LANA chromosome binding in episome persistence. *J. Virol.* **83**, 4326–4337 (2009).
38. E. De León Vázquez, K. M. Kaye, The internal Kaposi's sarcoma-associated herpesvirus LANA regions exert a critical role on episome persistence. *J. Virol.* **85**, 7622–7633 (2011).
39. F. Juillard, E. De León Vázquez, M. Tan, S. Li, K. M. Kaye, Kaposi's Sarcoma-associated herpesvirus LANA-adjacent regions with distinct functions in episome segregation or maintenance. *J. Virol.* **93**, e02158-18 (2019).
40. Q. Sun *et al*., Kaposi's sarcoma-associated herpesvirus LANA recruits the DNA polymerase clamp loader to mediate efficient replication and virus persistence. *Proc. Natl. Acad. Sci. U.S.A.* **111**, 11816–11821 (2014).
41. J. H. Jeong *et al*., Regulation and autoregulation of the promoter for the latency-associated nuclear antigen of Kaposi's sarcoma-associated herpesvirus. *J. Biol. Chem.* **279**, 16822–16831 (2004).
42. J. Friborg Jr., W. Kong, M. O. Hottiger, G. J. Nabel, p53 inhibition by the LANA protein of KSHV protects against cell death. *Nature* **402**, 889–894 (1999).
43. W. Chen, I. B. Hilton, M. R. Staudt, C. E. Burd, D. P. Dittmer, Distinct p53, p53:LANA, and LANA complexes in Kaposi's sarcoma-associated herpesvirus lymphomas. *J. Virol.* **84**, 3898–3908 (2010).
44. S. Santag *et al*., Recruitment of the tumour suppressor protein p73 by Kaposi's sarcoma herpesvirus latent nuclear antigen contributes to the survival of primary effusion lymphoma cells. *Oncogene* **32**, 3676–3685 (2012).
45. S. R. Grossman, p300/CBP/p53 interaction and regulation of the p53 response. *Eur. J. Biochem.* **268**, 2773–2778 (2001).
46. C. Lim, Y. Gwack, S. Hwang, S. Kim, J. Choe, The transcriptional activity of cAMP response element-binding protein-binding protein is modulated by the latency-associated nuclear antigen of Kaposi's sarcoma-associated herpesvirus. *J. Biol. Chem.* **276**, 31016–31022 (2001).
47. A. Gupta, D. G. Oldenburg, E. Salinas, D. W. White, J. C. Forrest, Murine gammaherpesvirus 68 expressing Kaposi sarcoma-associated herpesvirus latency-associated nuclear antigen (LANA) reveals both functional conservation and divergence in LANA homologs. *J. Virol.* **91**, e00992-17 (2017).
48. R. Marmorstein, M. M. Zhou, Writers and readers of histone acetylation: Structure, mechanism, and inhibition. *Cold Spring Harb. Perspect. Biol.* **6**, a018762 (2014).
49. Y. Li *et al*., Accurate in silico identification of species-specific acetylation sites by integrating protein sequence-derived and functional features. *Sci. Rep.* **4**, 5765 (2014).
50. Z. H. Davis *et al*., Global mapping of herpesvirus-host protein complexes reveals a transcription strategy for late genes. *Mol. Cell* **57**, 349–360 (2015).
51. G. Sarek *et al*., Reactivation of the p53 pathway as a treatment modality for KSHV-induced lymphomas. *J. Clin. Invest.* **117**, 1019–1028 (2007).
52. M. Shamay *et al*., A protein array screen for Kaposi's sarcoma-associated herpesvirus LANA interactors links LANA to TIP60, PP2A activity, and telomere shortening. *J. Virol.* **86**, 5179–5191 (2012).
53. M. Shamay, A. Krithivas, J. Zhang, S. D. Hayward, Recruitment of the de novo DNA methyltransferase Dnmt3a by Kaposi's sarcoma-associated herpesvirus LANA. *Proc. Natl. Acad. Sci. U.S.A.* **103**, 14554–14559 (2006).
54. S. C. Verma, Q. Cai, E. Kreider, J. Lu, E. S. Robertson, Comprehensive analysis of LANA interacting proteins essential for viral genome tethering and persistence. *PLoS One* **8**, e74662 (2013).
55. F. Lu *et al*., Identification of host-chromosome binding sites and candidate gene targets for Kaposi's sarcoma-associated herpesvirus LANA. *J. Virol.* **86**, 5752–5762 (2012).
56. H. J. Kwun *et al*., Kaposi's sarcoma-associated herpesvirus latency-associated nuclear antigen 1 mimics Epstein-Barr virus EBNA1 immune evasion through central repeat domain effects on protein processing. *J. Virol.* **81**, 8225–8235 (2007).
57. H. J. Kwun *et al*., The central repeat domain 1 of Kaposi's sarcoma-associated herpesvirus (KSHV) latency associated-nuclear antigen 1 (LANA1) prevents cis MHC class I peptide presentation. *Virology* **412**, 357–365 (2011).
58. A. Zaldumbide, M. Ossevoort, E. J. Wiertz, R. C. Hoeben, In cis inhibition of antigen processing by the latency-associated nuclear antigen I of Kaposi sarcoma herpes virus. *Mol. Immunol.* **44**, 1352–1360 (2007).
59. Y. Yin, B. Manoury, R. Fåhraeus, Self-inhibition of synthesis and antigen presentation by Epstein-Barr virus-encoded EBNA1. *Science* **301**, 1371–1374 (2003).
60. J. Levitskaya, Inhibition of antigen processing by the internal repeat region of the Epstein-Barr virus nuclear antigen-1. *Nature* **375**, 685–688 (1995).
61. R. Ponnusamy *et al*., KSHV but not MHV-68 LANA induces a strong bend upon binding to terminal repeat viral DNA. *Nucleic Acids Res.* **43**, 10039–10054 (2015).
62. K. J. Barnum, M. J. O'Connell, Molecular mechanisms involved in initiation of the DNA damage response. *Mol. Cell. Oncol.* **2**, e970065 (2015).
63. A. Liu, K. Yoshioka, V. Salerno, P. Hsieh, The mismatch repair-mediated cell cycle checkpoint response to fluorodeoxyuridine. *J. Cell. Biochem.* **105**, 245–254 (2008).

Downloaded at Universidade Católica Portuguesa on November 13, 2020